Sensing Behavior Study of Manganese Zinc Ferrite Nanoparticles Against Carbon Tetrachloride at Various Temperatures

Gholam Reza Aboutalebi[1], Hamid Reza Ebrahimi[2], Hossein Emami[3], Saeid Daneshmand[4], Gholam Reza Amiri[5]

1- Department of Electrical Engineering, Majlesi Branch, Islamic Azad University, Majlesi, Isfahan 9631656769, Iran.
Email: gh.r.aboutalebi@gmail.com

2- - Advanced Engineering Research Center, Majlesi Branch, Islamic Azad University, Majlesi, Isfahan, Iran,
Email: hebrahimi2010@gmail.com (Corresponding author)

3- Department of Electrical Engineering, Majlesi Branch, Islamic Azad University, Majlesi, Isfahan 9631656769, Iran.
Email: h.emami@iaumajlesi.ac.ir

4- Department of Mechanical Engineering, Majlesi Branch, Islamic Azad University, Majlesi, Isfahan 9631656769, Iran.
Email: saeed_daneshmand@yahoo.com

5- Department of Physics, Falavarjan Branch, Islamic Azad University, Isfahan, Iran.
Email: amiri.nano@gmail.com

Received: June 2022 Revised: July 2022 Accepted: August 2022

ABSTRACT:
In this study, zinc ferrite nanoparticles with a diameter of less than 50 nm were synthesized. Using XRD (X-ray Diffraction), Scanning Electron Microscope (SEM) and Transmission Electron Microscope (TEM) the morphology and structure of this ferrite was investigated. The formation of spinel phase in Zn-Mn ferrite was shown by X-ray analysis. SEM photograph has shown spherical shape of nanoparticles and the dimensions of the samples were confirmed by Transmission Electron Microscope (TEM) at the nanoscale. Using the Debye-Scherrer formula, the size of Mn ferrite nanoparticle crystals was calculated to be about 13 nm. To check the properties related to the sensitivity of this ferrite, a fully insulated Plexiglass box was used and placed in it. By injecting 1 mL of liquid and vapor it, we will have 200 ppm concentration of each sample in this box. Then the injected vapored sample in this box is exposed to the ferrite. After this step, the conductivity of the ferrite in a closed circuit was changed. By changing the sample type, amount of this conductivity was varied. Five gases were tested in this project: ethanol, dimethyl formamid, carbon tetrachloride, acetonitrile and acetone. Among these samples the carbon tetrachloride had the best sensitivity performance. Finally, the sensor equation for carbon tetrachloride was extracted by applying different concentrations of it from 20 to 200 ppm.

KEYWORDS: Carbon Tetrachloride Sensor, Ferrite, Gas Sensor, Manganese Zinc Ferrite Nanoparticle, Sensitivity, X–ray Diffraction.

1. INTRODUCTION

Nanoscale metal oxide sensors show good sensitivity and selectivity in detecting gases [1-7].

Therefore, by using different metal oxides, we will have a wide range of materials for this purpose. Nanostructured materials offer new ways to improve and enhance the properties and efficiency of gas sensors due to their much higher surface materials compared to micro and macro grained materials [8-14]. Hence, due to the increased sensitivity of nanostructured sensors, these types of sensors respond much faster for specific gas detection applications [15-20].

Previous studies regarding the use of manganese and zinc ferrite as gas sensor materials include ZnO to LPG [21], manganese zinc ferrite nano particles to ethanol [22], zinc copper ferrite nanocomposites to LPG and CO2 [23], zinc copper ferrite nanoparticles to LPG [24], ZnO to formaldehyde [25] and manganese nickel ferrite nanoparticles to humidity [26].

Nano ferrites are synthesized in various methods [27-34], but in this study we applied an effective

Paper type: Research paper
DOI: https:// 10.30486/mjee.2022.696509
How to cite this paper: Gh. R. Aboutalebi, H. R. Ebrahimi, H. Emami, S. Daneshmand and Gh. R. Amiri, **"Sensing Behavior Study of Manganese Zinc Ferrite Nanoparticles Against Carbon Tetrachloride at Various Temperatures"**, Majlesi Journal of Electrical Engineering, Vol. 16, No. 3, pp. 85-89, 2022.

co-precipitation method.

Nano sized manganese zinc ferrites are found to exhibit interesting gas sensing properties. These nano particles are responded to different gases Such as ethanol, dimethyl formamid, carbon tetrachloride, acetonitrile and acetone. Among these gases, carbon tetrachloride shows the best full response at all examining temperatures.

2. EXPERIMENTAL

2.1. $Mn_{0.5}Zn_{0.5}Fe_2O_4$ nanoparticles Synthesis

At first, zinc chloride, manganese chloride and ferric chloride solutions, by the molar ratio of 1:1:4 were dissolved in double-distilled water. The zinc chloride and manganese chloride solutions were slowly added dropwise to ferric chloride solution for 10 minutes. After that, 8M saturated NaOH solution was added until the pH of the solution reached 12. Manganese zinc ferrite nanoparticles began to precipitate in the solution and the resulting mixture was stirred for 30 minutes by a magnetic stirring device. After stirring, the resulting mixture was filtered through a soft filter and the obtained powder was washed several times with distilled water, and each time the conductivity of the washing solution was measured until its conductivity reached less than 50μS/Cm. Then the powder was dried at 100 degrees Celsius. After this step, the sample was heated for 3 hours at a temperature of 500 degrees Celsius in the furnace.

$$0.5MnCl_2+0.5ZnCl_2+2FeCl_3+8NaOH \rightarrow Mn_{0.5}Zn_{0.5}Fe_2O_4 + 8NaCl + 4H_2O \quad (1)$$

X-ray diffraction (XRD) patterns on Bruker D8 Advance X-ray diffractometer with Cu Ka anode (λ=0.1542 nm), SEM (scanning electron microscope) and TEM (transmission electron microscope) were used to analyze the particle size distribution.

Scherer's equation was used to calculate the structural coherence length:

$$D = 0.9\ \lambda / \beta\ Cos\theta \quad (2)$$

In this equation, D is the crystal size in nanometers, λ is the wavelength of Cu-Kα and is equal to 0.154 nm, β is the half width of the peak in radians (instrumental line width subtracted) and θ is the corresponding diffraction angle.

2.2. Interface Preparation

Similar to Fig. 1 to prepare the sensor tablet and interface parts, first, two copper conductor wires with a thickness of 0.2 mm were placed on the mica insulation surface with a diameter of 1.4 cm in a E shape. Then, 0.2 grams of $Mn_{0.5}Zn_{0.5}Fe_2O_4$ nano-powder ferrite, which has been calcined at 500 degrees Celsius, was pressed on the insulation surface with a manual press for 30 minutes. Pressing was done at a pressure of 600 kg/m2.

In Fig. 2, schematic cross section of applied interface from two, right side and left side view is presented. The output copper wires were connected to a resistant circuit.

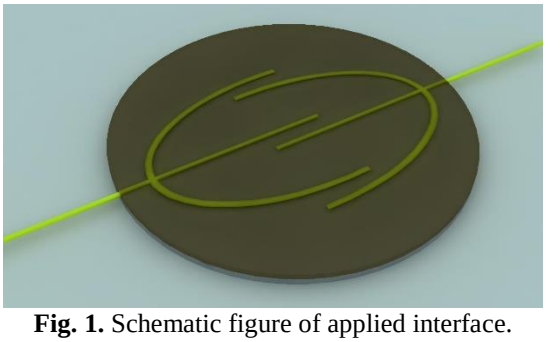

Fig. 1. Schematic figure of applied interface.

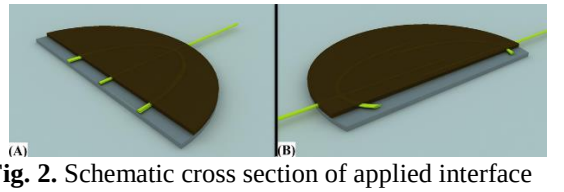

Fig. 2. Schematic cross section of applied interface from two (A), right side and (B), left side view.

3. RESULTS AND DISCUSSION

3.1. Particle Size Determination

XRD patterns of $Mn_{0.5}Zn_{0.5}Fe_2O_4$ ferrite nanoparticles are shown in Fig. 3. As can be seen in the figure, all the samples are single phase and have spinel-ferrite structure. In addition, the average particle size determined by the Debye-Scherer formula is 13nm.

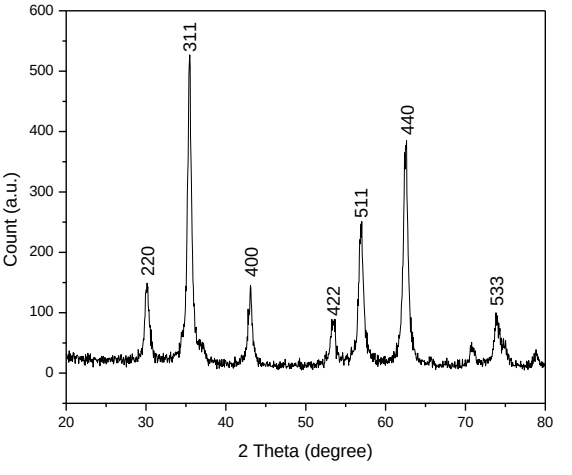

Fig. 3. XRD pattern of the $Mn_{0.5}Zn_{0.5}Fe_2O_4$ nano particles.

The grain size and surface morphology of the material were obtained by scanning electron microscopy. The SEM image of $Mn_{0.5}Zn_{0.5}Fe_2O_4$ ferrite nanoparticles is shown in Fig. 4. Based on this picture, the size of nanoparticles is 18×19×25 nm.

It is evident from this figure that the particles of $Mn_{0.5}Zn_{0.5}Fe_2O_4$ nanoparticles have a random orientation. However, the packed structure with pores is observed in it. The observed pores are responsible for absorbing the target gas. The clustering of particles in the shape is continuously reduced and therefore the porosity increases and the grain size is reduced, which was confirmed by XRD analysis.

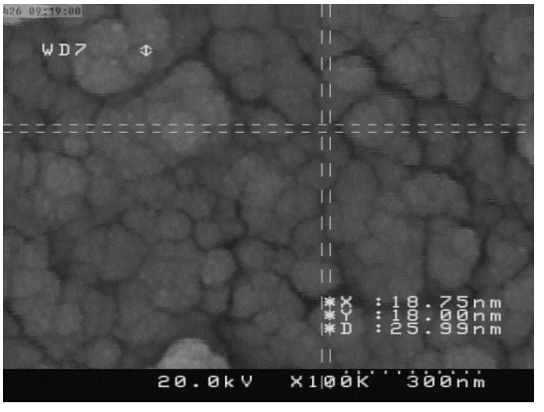

Fig. 4. SEM image of $Mn_{0.5}Zn_{0.5}Fe_2O_4$ nano particles.

The TEM photo of $Mn_{0.5}Zn_{0.5}Fe_2O_4$ sample is shown in Fig. 5. As can be seen, the size distribution is almost in the entire photograph, which means that the synthesis method is suitable. In addition, the size of the particles in this photo was determined below 20 nm.

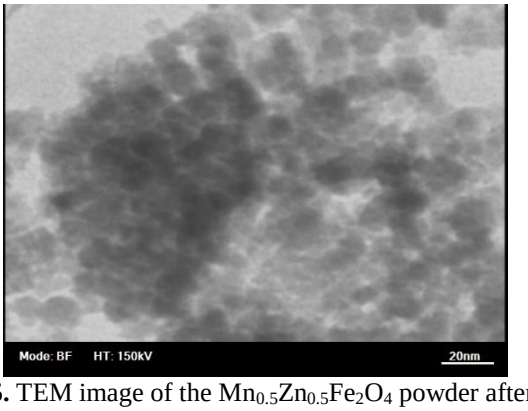

Fig. 5. TEM image of the $Mn_{0.5}Zn_{0.5}Fe_2O_4$ powder after 3 hours heating at 500ºC.

3.2. Gas Sensor Process

In this sensor, the resistance changes when exposed to different gases, and also the amplitude of resistant changes in the defferent gas concentration. The diagram of variation of the sensor sensitivity against different gases for different temperatures of the sensor substrate is shown in Fig. 6.

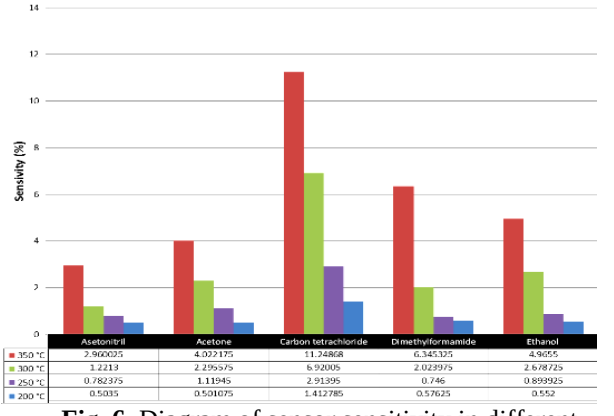

Fig. 6. Diagram of sensor sensitivity in different substrate temperatures (exposed with 5 different gases).

4. CONCLUSION

The $Mn_{0.5}Zn_{0.5}Fe_2O_4$ was synthesized by simple co-precipitation method. The nano particle sizes were determined a few nanometers (less than 20 nm). This size was confidence by XRD and TEM studies. In XRD pattern according Debye-Scherrer's equation, the mean particle size is 13 nm. The TEM image confirms the manganese zinc ferrite nanoscale formation on glass surface.

A sensor interface was prepared to check the sensitivity. This interface was exposed to five gases, ethanol, dimethylformamide, carbon tetrachloride, acetonitrile and acetone. The best response was obtained for carbon tetrachloride. Finally, the sensor equation for carbon tetrachloride in the concentration range between 20-200 ppm was derived.

5. ACKNOWLEDGEMENTS

In this study, the laboratory facilities and equipment of Islamic Azad University, Majlesi branch were used, and the authors are grateful for the cooperation of the officials of this university.

REFERENCES

[1] Huang, X. J., Choi, Y. K., **"Chemical sensors based on nanostructured materials."**, *Sensor Actuat. B-Chem.*, Vol. 122, pp. 659–671, 2007.

[2] N.V. Hoang, C.M. Hung, N.D. Hoa, N.V. Duy, N.V. Hieu, **"Facile on-chip electrospinning of $ZnFe_2O_4$ nanofiber sensors with excellent sensing performance to H_2S down ppb level"**, *J. Hazard Mater.*, Vol. 360, pp. 6–16, 2018.

[3] T. Saidi, O. Zaim, M. Moufid, N.E. Bari, R. Ionescu, B. Bouchikhi, **"Exhaled breath analysis using electronic nose and gas chromatography-mass spectrometry for non-invasive diagnosis of chronic**

kidney disease, diabetes mellitus and healthy subjects", *Sens. Actuators, B*, Vol. 257, pp. 178–188, 2018.

[4] T. Vidya Sagar, T. Subba Rao, K. Chandra Babu Naidu, **"AC-electrical conductivity, magnetic susceptibility, dielectric modulus and impedance studies of sol-gel processed nano-NiMgZn ferrites"**, *Materials Chemistry and Physics*, Vol. 258, 2021, 123902.

[5] W. -J. Zhao, K. -L. Ding, Y. -S. Chen, F. -Y. Xie and D. Xu, **"Optimized Low Frequency Temperature Modulation for Improving the Selectivity and Linearity of SnO2 Gas Sensor,"** *in IEEE Sensors Journal*, Vol. 20, No. 18, pp. 10433-10443, 15 Sept.15, 2020.

[6] Zarzycki, A.; Chojenka, J.; Perzanowski, M.; Marszalek, M. **"Electrical Transport and Magnetic Properties of Metal/Metal Oxide/Metal Junctions Based on Anodized Metal Oxides"**. *Materials* 2021, 14, 2390.

[7] Gautam Yogendra K., Sharma Kavita, Tyagi Shrestha, Ambedkar Anit K., Chaudhary Manika and Pal Singh Beer, **"Nanostructured metal oxide semiconductor-based sensors for greenhouse gas detection: progress and challenges."** 2021.

[8] Fang, C., Li, H., Li, L., Su, H., Tang, J., Bai, X. and Liu, H. (2022), **"Smart Electronic Nose Enabled by an All-Feature Olfactory Algorithm."**, *Adv. Intell. Syst.* 2200074.

[9] Skotadis, E.; Aslanidis, E.; Kainourgiaki, M.; Tsoukalas, D. **"Nanoparticles Synthesised in the Gas-Phase and Their Applications in Sensors: A Review."** *Appl. Nano* 2020, 1, pp. 70-86, 2020.

[10] Korotcenkov, G. **"Current Trends in Nanomaterials for Metal Oxide-Based Conductometric Gas Sensors: Advantages and Limitations. Part 1: 1D and 2D Nanostructures."**, *Nanomaterials 2020*, 10, 1392.

[11] Zamiri, G.; Haseeb, A.S.M.A. **"Recent Trends and Developments in Graphene/Conducting Polymer Nanocomposites Chemiresistive Sensors."** *Materials 2020*, 13, 3311.

[12] Wei Wang, Yirui Shu, Hengli Xiang, Dehua Xu, Pan Zhang, Genkuan Ren, Yanjun Zhong, Xiushan Yang, **"Magnetic properties of $Cu_{0.5}Mg_{0.5}Fe_2O_4$ nanoparticles synthesized with waste ferrous sulfate"**, *Materials Today Communications*, Vol. 25, 2020, 101516.

[13] Abdolrahim Yousefi-Darani, Majharulislam Babor, Olivier Paquet-Durand, Bernd Hitzmann, **"Model-based calibration of a gas sensor array for on-line monitoring of ethanol concentration in Saccharomyces cerevisiae batch cultivation"**, *Biosystems Engineering*, Vol. 198, pp. 198-209, 2020.

[14] Nikolic, M.V.; Milovanovic, V.; Vasiljevic, Z.Z.; Stamenkovic, Z. **"Semiconductor Gas Sensors: Materials, Technology, Design, and Application"**. *Sensors 2020*, 20, 6694.

[15] Chen, N. S., Yang, X. J., Liu, E. S., Huang, J. L., **"Reducing gas-sensing properties of ferrite compounds MFe_2O_4 (M=Cu, Zn, Cd and Mg)."**, *Sensor Actuat. B-Chem.*, Vol. 66, pp. 178-180, 2000.

[16] Kumar, Y., Sharma, A., Shirage, P.M., **"Shape-controlled $CoFe_2O_4$ nanoparticles as an excellent material for humidity sensing."**, *RSC Adv.*, 2017, Vol. 7(88), pp. 55778–55785, 2017.

[17] Singh, A., Singh, R., Singh, S., Tandon Yadav, B.C., **"Preparation and characterization of nanocrystalline nickel ferrite thin films for development of a gas sensor at room temperature."**, *J. Mater. Sci.: Mater. Electron.*, 2016, Vol. 27(8), pp. 8047–8054, 2016.

[18] Koli, P.B., Kapadnis, K.H., Deshpande, U.G., **"Methanol gas sensing properties of pervoskite $LaFeO_3$ nanoparticles doped by transition metals Cr_3+ and Co_2+."**, *J. Chem. Pharm. Res.*, Vol. 9(1), pp. 253–259, 2017.

[19] Rong, Q., Zhang, Y., Wang, C., Zhu, Z., Zhang, J., Liu, Q., **"A high selective methanol gas sensor based on molecular imprinted Ag–$LaFeO_3$ fibers."**, *Sci. Rep.*, 2017, 7, 12110.

[20] Satyanarayana, L., Reddy, K. M., Manorama, S. V., **"Synthesis of nanocrystalline $Ni_{1-x}Co_xMn_xFe_{2-x}O_4$: a material for liquefied petroleum gas sensing. Sensor"**, *Actuat. B-Chem.*, Vol. 89, pp. 62-67, 2003.

[21] Ladhea, R. D., Guravc, K. V., Pawarb, S. M., Kimc, J. H., Sankapal, B. R., **"p-PEDOT: PSS as a heterojunction partner with n-ZnO for detection of LPG at room temperature."**, *J. Alloy Compd.*, Vol. 515, pp. 80–85, 2012.

[22] Kadu, A. V., Jagtap, S. V., Chaudhari, G. N., **Studies on the preparation and ethanol gas sensing properties of spinel $Zn_{0.6}Mn_{0.4}Fe_2O_4$ nanomaterials."**, *Current Applied Physics*, Vol. 9, pp. 1246–1251, 2009.

[23] Singh, A., Singh, S., Joshia, B. D., Shukla, A., Yadav, B. C. Tandon, P., **"Synthesis, characterization, magnetic properties and gas sensing applications of $Zn_xCu_{1-x}Fe_2O_4$ ($0.0 \leq x \leq 0.8$) nanocomposites."**, *Mat. Sci. Semicon. Proc.*, Vol. 27, pp. 934–949, 2014.

[24] Jain,A., Baranwal, R. K., Bharti, A., Vakil, Z., Prajapati, C. S,. **"Study of Zn-Cu Ferrite Nanoparticles for LPG Sensing."**, *The Scientific World Journal*, Vol. 2013, Article ID 790359, 7 pages

[25] Qiaohua, F., Ruru, Z., Xintian, M., Yunbo, S., **"Preparation of ZnO Semiconductor Formaldehyde Gas Sensor."**, *2013 2nd International Conference on Measurement, Information and Control*.

[26] Köseoglu, Y., Aldemir, I., Bayansal, F., Kahraman, S., Çetinkara, H. A., **"Synthesis, characterization and humidity sensing properties of $Mn_{0.2}Ni_{0.8}Fe_2O_4$ Nanoparticles."**, *Mater. Chem. Phys.*, Vol. 139, pp. 789-793, 2013.

[27] Shan, J., Bougiatioti, P., Liang, L., Reiss, G., Kuschel, T., van Wees, B.J. **"Nonlocal magnon spin transport in $NiFe_2O_4$ thin films."**, *Appl. Phys. Lett.*, Vol. 110(13), 132406 (1–5), 2017.

[28] Chavan, P., Naik, L.R. **"Investigation of energy band gap and Conduction mechanism of magnesium substituted nickel ferrite nanoparticles."**, *Phys. Status Solid A*, Vol. 214(9), pp. 1–8, 2017.

[29] Babadi, N., Tavakkoli, H., Afshari, M., **"Synthesis and characterization of nanocomposite $NiFe_2O_4$@SalenSi and its application in efficient removal of Ni(II) from aqueous solution."**, *Bull. Chem. Soc. Ethiop*., Vol. 32(1), pp. 77–88, 2018.

[30] Pubby, K., Meena, S.S., Yusuf, S.M., Narang, S.B., **"Cobalt substituted nickel ferrites via Pechini's sol–gel citrate route: X-band electromagnetic characterization."**, *J. Magn. Magn. Mater*., Vol. 466, pp. 430–445, 2018.

[31] Ananya Dey, **"Semiconductor metal oxide gas sensors: A review"**, *Materials Science and Engineering: B*, Vol. 229, pp. 206-217, 2018.

[32] Sendi et al., **"Performance of MOX Gas Sensors Obtained by Mixing P-Type and N-Type Metal Oxides for Relaible Indoor Air Quality Monitoring,"** *2019 20th International Conference on Solid-State Sensors, Actuators and Microsystems & Eurosensors XXXIII (TRANSDUCERS & EUROSENSORS XXXIII)*, pp. 1305-1308, 2019.

[33] Feng, S.; Farha, F.; Li, Q.; Wan, Y.; Xu, Y.; Zhang, T.; Ning, H. **"Review on Smart Gas Sensing Technology."** *Sensors 2019*, Vol. 19, 3760, 2019.

[34] Ali Mirzaei, Jae-Hyoung Lee, Sanjit Manohar Majhi, Matthieu Weber, Mikhael Bechelany, Hyoun Woo Kim, and Sang Sub Kim, **"Resistive gas sensors based on metal-oxide nanowires"**, *Journal of Applied Physics 12*6, 241102 (2019).